Proceedings of the 11th ICPMG 2026
11th International Conference on Physical Modelling in Geotechnics
8-12 June 2026, Zurich, Switzerland

Model tests on bearing capacity of soil cement H-shaped steel piles with headed studs in sand under confining pressure

Natsumi Tomita
Taisei Advanced Center of Technology, Yokohama, Japan, kndntm00@pub.taisei.co.jp

Keita Shibata, Yoshihiro Horii, Toru Watanabe,
Taisei Advanced Center of Technology, Yokohama, Japan, sbtkit00@pub.taisei.co.jp, horii@arch.taisei.co.jp, toru.watanabe@sakura.taisei.co.jp

Shuhei Otsuka
Institute of Science Tokyo, Tokyo, Japan, ootsuka.s.86ed@m.isct.ac.jp

Yuto Nomura, Shuichi Shimomura
Nihon Univercity, Narashino, Japan, ciyt24020@g.nihon-u.ac.jp, shimomura.shuichi@nihon-u.ac.jp

ABSTRACT: To reuse soil–cement retaining walls originally constructed as temporary earth-retaining structures as permanent soil–cement H-shaped steel piles, it is necessary to evaluate their load-bearing performance. Because of the relatively low strength of soil–cement, headed studs are commonly installed on the H-shaped steel core to enhance the bearing capacity. In this study, vertical loading tests were conducted on soil–cement H-shaped steel piles using a pressurised soil chamber to simulate ground confinement, with particular focus on the effect of headed studs on the vertical bearing capacity. The test results confirmed that the installation of headed studs affects the failure mode of the soil–cement and enhances the increase in bearing capacity induced by ground confinement.

1 INTRODUCTION

In recent years, methods have been developed to reuse soil–cement walls originally constructed as temporary retaining structures as permanent foundation piles to reduce construction costs and environmental impact. These walls consist of H-shaped steel sections (hereafter referred to as the steel core) and soil–cement, through which vertical loads are transferred from the steel to the ground (Figure 1).

Because the strength of soil–cement is relatively low, its failure mechanism is complex, and evaluating the bearing capacity—determined by the failure at the interface between the steel core and soil–cement—is particularly important. The vertical load transmitted from the steel core is resisted by adhesion at the steel core soil–cement interface (comprising cohesion and friction), shear resistance of the soil–cement, and bearing resistance below the steel core tip.

Since soil–cement walls are confined by the surrounding ground, their load-bearing performance is affected by ground confinement. Kiritani et al. (2025) conducted vertical loading tests using a pressurised soil chamber and demonstrated that bearing capacity increased with increasing overburden pressure. When used as permanent piles, headed studs (hereafter referred to as studs) are generally installed on the steel core. Previous studies on the effect of studs have mainly been based on in-situ loading tests (Mano,

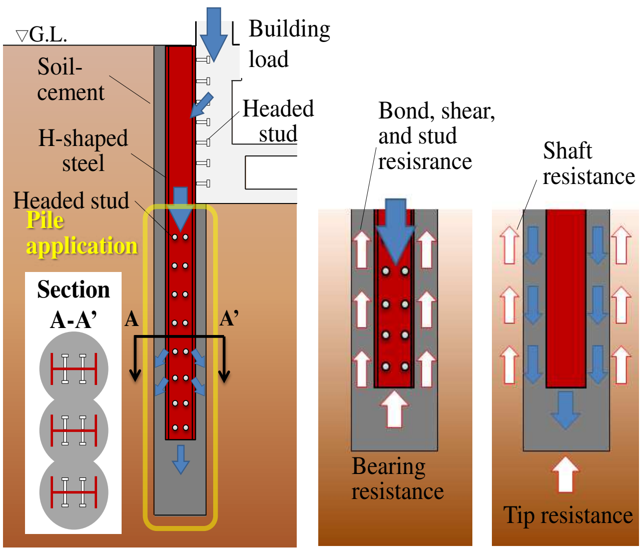

Figure 1. Conceptual illustration of the vertical bearing mechanism of soil–cement H-shaped steel pile, including bond resistance along the steel core, shear resistance of the soil–cement, tip bearing resistance, and resistance provided by headed studs.

2018; Taya, 2021) or model tests using acrylic or steel cylinders (Satake, 2003; Watanabe, 2021). To the authors' knowledge, no studies have quantitatively evaluated the influence of ground confinement on permanent piles with installed studs.

In this study, composite pile specimens consisting of a steel core and soil–cement (hereafter referred to as H-shaped steel piles)—were subjected to vertical loading tests under confined and unconfined condition (with/without a pressurised soil chamber). The effects of stud installation and ground confinement on the failure behaviour and vertical bearing capacity were investigated.

2 OUTLINE OF EXPERIMENTS

2.1 Experimental methods and conditions

Two types of vertical loading tests were conducted: tests using a pressurised soil chamber to simulate ground confinement; and unconfined tests conducted for comparison. The experimental cases are summarised in Table 1, and the geometry of the model piles is shown in Figure 2.

Cases beginning with "U" denote unconfined conditions, whereas "TL" and "TM" correspond to overburden pressures of 50 and 100 kPa, respectively, representing confined ground conditions. These pressures correspond to ground depths of approximately 5 and 10 m below the foundation level. The numerical suffix in each case name indicates the number of stud rows.

Two types of model piles were fabricated: piles without studs and ones with three rows of studs. The model scale was approximately 1/2.5 of the prototype. The steel core was an H-shaped steel section (H-175 × 90 × 5 × 7 mm). The soil–cement portion had a diameter of 250 mm, a bond length of 400 mm with the steel core, and an extension of 350 mm below the steel core tip.

Table 1. Test cases.

Overburden pressure p_0(kPa)	Without studs		With studs	
	Case	q_u (N/mm^2)	Case	q_u (N/mm^2)
Unconfined	U_10C0	0.82	U_10C3	0.76
50	TL_10C0	0.92	TL_10C3	0.84
100	TM_10C0	0.90	TM_10C3	0.87

Table 2. Soil cement mix proportion.

q_{u0} (N/mm^2)	Test soil		Cement slurry		
	Fines content (%)	Water content (%)	Additive ratio (%)	W/C (%)	Bentonite (%)
0.5	20	23	15	70	0.5
1.0			19	64	0.5

The soil–cement mix proportions are listed in Table 2. The target unconfined compressive strength (q_{u0}) was set to 1.0 N/mm². The measured unconfined compressive strength of the specimens q_u prepared during model fabrication are also shown in Table 1.

To examine the dependency of soil–cement strength on confining pressure, triaxial compression tests were conducted. In addition to the mix used in the model pile tests with q_{u0}=1.0N/mm², specimens prepared with a mix corresponding to q_{u0}=0.5 N/mm² were also tested under confining pressures ranging from 50 to 200 kPa. The mix with q_{u0} =0.5 N/mm² is also listed in Table 2. As shown in Figure 3, the strength showed a slight increasing trend with increasing confining pressure.

2.2 Fabrication procedure of model piles

The fabrication procedure for the model piles was as follows.

1. An acrylic plate with an opening matching the steel core cross-section was fixed to the lower end of a cylindrical void form with a diameter of 250 mm.
2. The steel core was inserted, and the gap was sealed to prevent leakage.
3. The assembly was placed on a curing stand with the pile head facing downward (Figure 4).
4. JIS silica sand No. 5 and Tochigi clay were dry-mixed, after which tap water was added and kneaded to prepare the test soil.
5. A solidifying agent and bentonite were mixed with tap water to prepare a cement slurry.

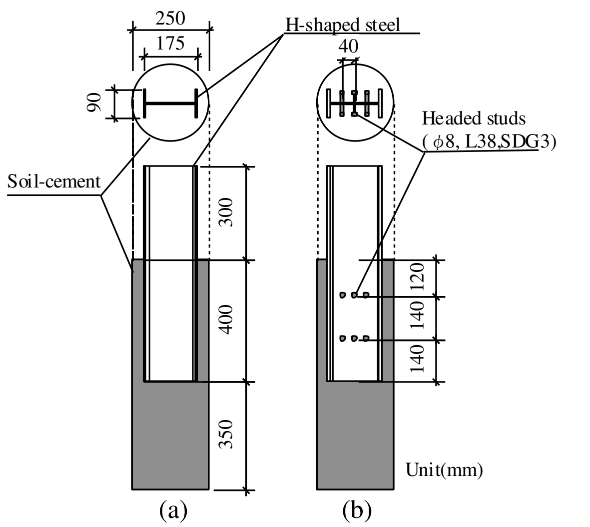

Figure 2. Shape of model pile. (a) Non-studded piles (U_10C0, TL_10C0 and TM_10C0), (b) Studded piles (U_10C3, TL_10C3 and TM_10C3).

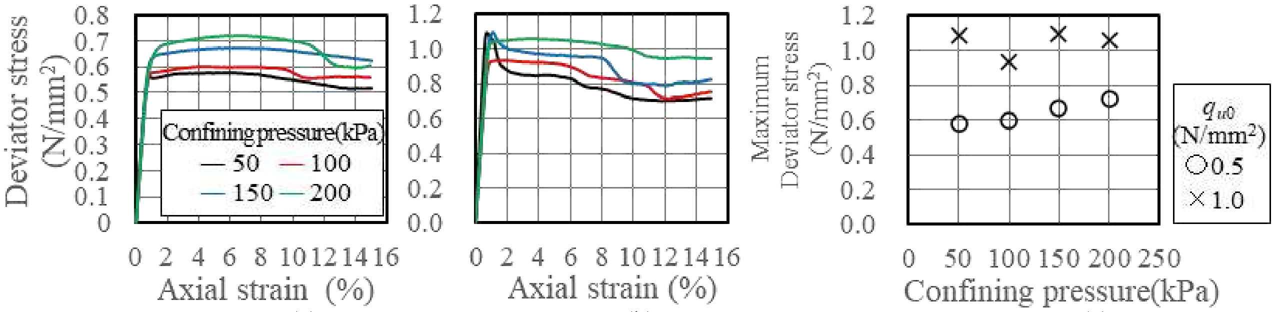

(a) (b) (c)

Figure 3. Triaxial compression test results for soil–cement specimens with target unconfined compressive strengths (q_{u0}) of 0.5 and 1.0 N/mm² under confining pressures of 50–200 kPa. (a) Stress–strain curves for q_{u0}= 0.5 N/mm², (b) Stress–strain curves for q_{u0} = 1 N/mm²; (c) Relationship between Maximum deviator stress and confining pressure.

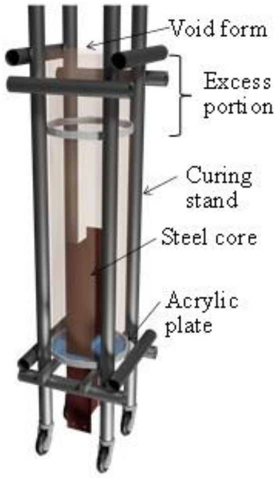

Figure 4. Model pile during fabrication and curing. The steel core was placed in a cylindrical void form and cured with the pile head facing downward.

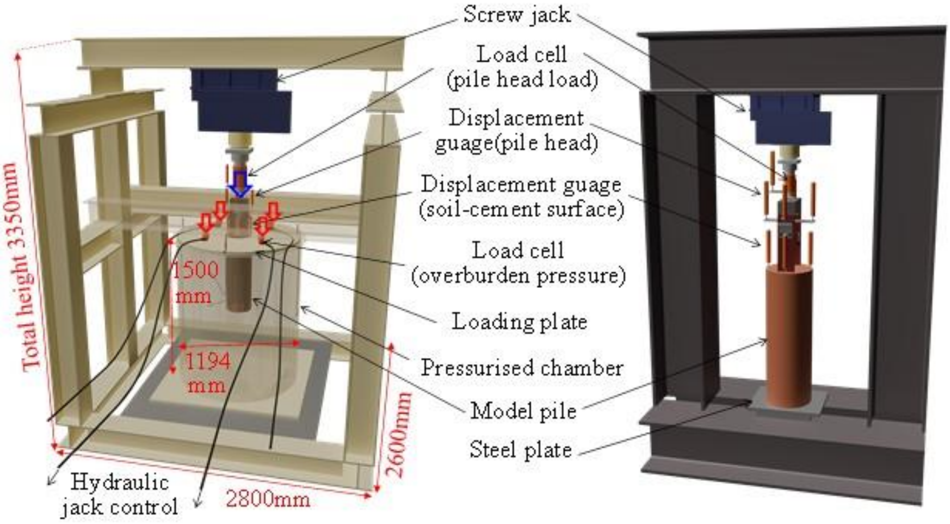

(a) (b)

Figure 5. Vertical loading test apparatus. Arrangement of the soil chamber, confining pressure system, model pile, loading device and instrumentation. (a) Under confined conditions, (b) Under unconfined conditions.

6. The test soil and the cement slurry were blended to form the soil−cement slurry, which was poured into the mould described in Step 1 and cured under sealed conditions at 20 °C for 14 days.

An excess length equivalent to 30 % of the soil−cement length was provided at the pile tip and trimmed off after curing.

2.3 Experimental apparatus and procedure

Figure 5 illustrates the vertical loading system and the pressurised soil chamber. The chamber was a steel cylinder with a diameter of 1,194 mm, a height of 1,500 mm and a wall thickness of 10 mm. To reduce wall friction, Teflon sheets coated with silicone grease were attached to the inner surface.

Tohoku silica sand No. 6 (ρ_s = 2.64, ρ_{dmax} = 1.68, ρ_{dmin} = 1.39 Mg/m³) with a grain-size distribution equivalent to JIS silica sand No. 5.5, was used to form the ground and prepared by air pluviation using a multiple-sieve device to achieve a relative density of 95 %. Shear strength parameters of the soil obtained from consolidated-drained triaxial tests were c = 13.6 kN/m² and φ = 44.6°.

Under confined conditions, the testing procedure was as follows:

1. Sand was first pluviated into the chamber to a depth of 750 mm below the ground level.
2. After levelling the sand surface, the model pile was installed at the center of the chamber, and sand was subsequently filled to the top of the chamber.
3. A rubber sheet and a rigid loading plate were placed on the sand surface.
4. Four load cells and four displacement transducers were mounted on the loading plate to monitor the

applied overburden pressure and surface settlement. Additional displacement transducers were set at the steel core head and at the top of the soil−cement to separately measure the displacement of each component. The overburden pressure was applied using four hydraulic jacks and maintained until ground settlement stabilised.

5. Vertical loading was subsequently applied by a screw jack aligned with the pile axis and controlled under displacement control at a rate of 1 mm/min. Loading was continued until a pile head displacement reached 25 mm, corresponding to 10% of the soil−cement diameter, after which unloading was performed. During loading, the target overburden pressure was controlled within ±5% by operating a hydraulic jack.
6. Following unloading, the surrounding sand was carefully excavated to observe the failure patterns of the pile body.

In the unconfined tests, the model piles were supported on a rigid steel plate directly without surrounding soil, and no overburden pressure was applied. Vertical loading was conducted under the same displacement-controlled conditions as those used in the confined tests.

After confirming pile failure and residual load behaviour, the vertical load was removed, and the pile was dismantled for failure observation. The differences observed between the confined and unconfined tests are therefore primarily attributed to the presence or absence of ground confinement, which governs the stress state and mobilisation of resistance in the soil−cement.

3 EXPERIMENTAL RESULTS

3.1 Relationship between pile head load and displacement

The relationships between the pile head load P and displacements at the steel core head S_P and the top of the soil−cement S_S are shown in Figures 6–8. In the figures, P_P denotes the pile head load at which the P−S_P relationship first exhibits a distinct change in slope. The difference between S_P and S_S (S_P−S_S) is defined as the relative displacement. P_R is defined the pile head load at a displacement of 25 mm (10% of the soil−cement diameter) and represents the residual strength. In cases where unloading was initiated before reaching 25 mm, P_R corresponds to the load just before unloading.

Under confined conditions, as shown in Figures 7 and 8, the non-studded piles (TL_10C0 and TM_10C0) reached P_P at a pile head displacement of approximately 1 mm, coinciding with the onset of relative displacement. After P_P, a slight load drop occurred, followed by a nearly constant load level. In contrast, for the studded piles (TL_10C3 and

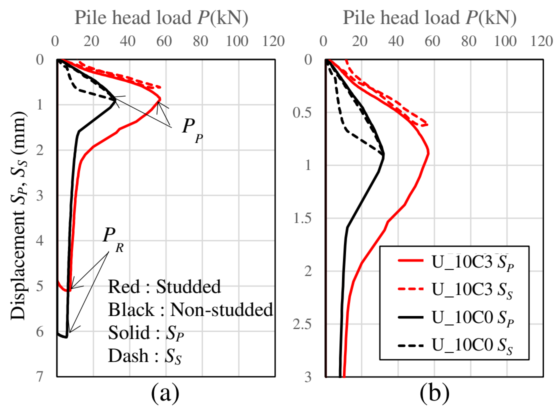

Figure 6. Relationship between pile head load and displacement under unconfined conditions. Results for non-studded pile (U_10C0) and studded pile (U_10C3). (a) Over view, (b) Enlarged view.

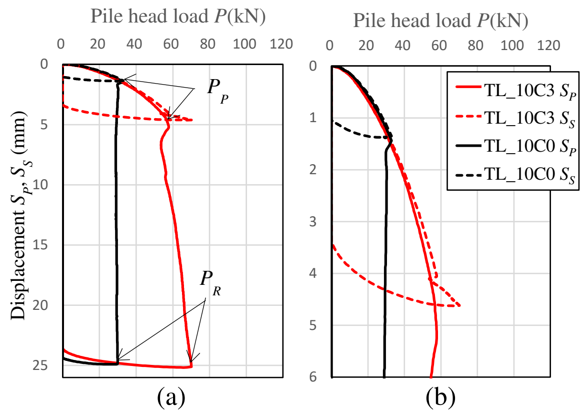

Figure 7. Relationship between pile head load and displacement under confined conditions with p_0=50kPa. Results for non-studded (TL_10C0) and studded piles (TL_10C3). (a) Over view, (b) Enlarged view.

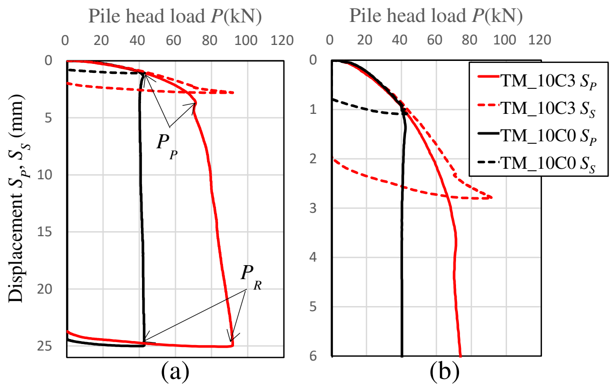

Figure 8. Relationship between pile head load and displacement under confined conditions with p_0=100kPa. Results for non-studded (TM_10C0) and studded piles (TM_10C3). (a) Over view, (b) Enlarged view.

TM_10C3), the pile head load continued increase even after P_P up to a displacement of 25mm, although the initial stiffness was almost identical to that of the non-studded piles. This behaviour clearly indicates the contribution of the headed studs to the post-peak load resistance under confined conditions. The ratios of P_R to P_P were 91 and 101% for non-studded piles (TL_10C0 and TM_10C0), and 121 and 129% for studded ones (TL_10C3 and TM_10C3), respectively.

Under unconfined conditions, the studded pile (U_10C3) showed higher initial stiffness and peak load than the non-studded one (U_10C0). However, the load decreased after P_P regardless of stud installation. These results indicate that the load increase beyond P_P due to studs occurs only under confined conditions.

In addition, unlike non-studded piles, studded piles reached P_P after onset of relative displacement. This behaviour is considered to be related to differences in failure modes, as discussed in the following section.

It should be noted that the unconfined tests were conducted to examine the presence or absence of ground confinement effects, and the bearing capacity obtained under unconfined conditions would be regarded as relatively conservative.

3.2 Failure behaviour

Two possible failure modes of the pile body are assumed: Mode I (bond failure along the steel core cross-section) and Mode II (combined bond-shear failure along the steel core-enveloping section), as shown in Figure 9, which are described in the Japanese recommendations for design of earth retaining structures (2017).

Figures 10−13 show sketches of surface cracks and the internal failure patterns observed after dismantling the piles.

In unconfined tests (U_10C0 and U_10C3), as shown in Figure 10, failure initiated on the soil−cement surface near the flange edges, where the cover thickness was smallest. Cracks propagated both upward and downward from the steel core tip depth, followed by horizontal cracks around the same depth.

In studded pile (U_10C3), additional cracks occurred along the stud depths, with wider crack openings and more severe damage compared with non-studded pile (U_10C0, Figure 10(b)).

For non-studded piles (U_10C0), bond failure occurred along the entire interface between the steel core and the soil−cement, corresponding to Mode I. Below the steel core tip, a wedge−shaped zone−likely formed by bearing of the soil−cement against the steel core cross-sectional shape–developed beneath the web and flange, from which splitting failure initiated (Figure 11(a)).

For studded piles (U_10C3), bond–shear failure developed below the upper studs accompanied by tensile cracks, corresponding to Mode II, whereas bond failure occurred above the upper studs (Figure 11(b)). Below the steel core tip, a wedge-shaped zone developed beneath the steel core-enveloping section, with splitting cracks propagating beneath the wedge (Figure 11(c)). Stud deformation and failure of the soil−cement beneath the studs were not clear, so it seemed that the steel core and the enclosed soil−cement moved together as an integrated unit. Thus, it was considered that the mechanical integrity improved by stud installation attributed to the higher initial stiffness (Figure 6).

Under confined conditions, as shown in Figure 12, the crack pattern became more localised with increasing overburden pressure. The studded piles (Figures 12(b) and (d)) exhibited more pronounced confinement effects.

In addition, for non-studded piles, separation along the interface between the steel core and the soil−cement could not be confirmed during manual disassembly, although relative displacement was observed (Figure 7, 8 and 13(a)). As not shown in the figures, no distinct wedge formation was observed below the steel core tip, and splitting failure

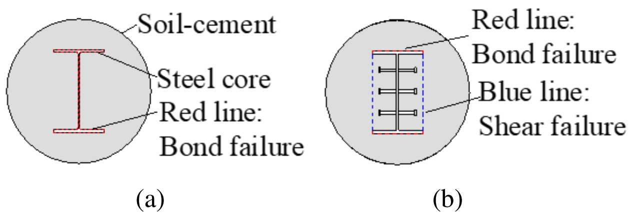

Figure 9. Failure mode. (a) Mode Ⅰ, (b) Mode Ⅱ.

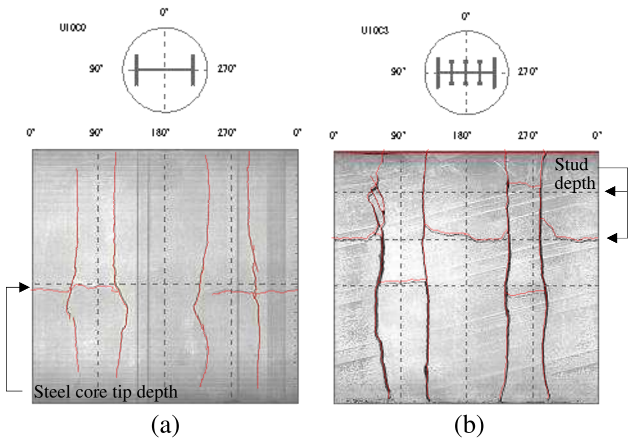

Figure 10. Crack sketches of model piles under unconfined conditions. (a) Non-studded pile (U_10C0), (b) Studded pile (U_10C3).

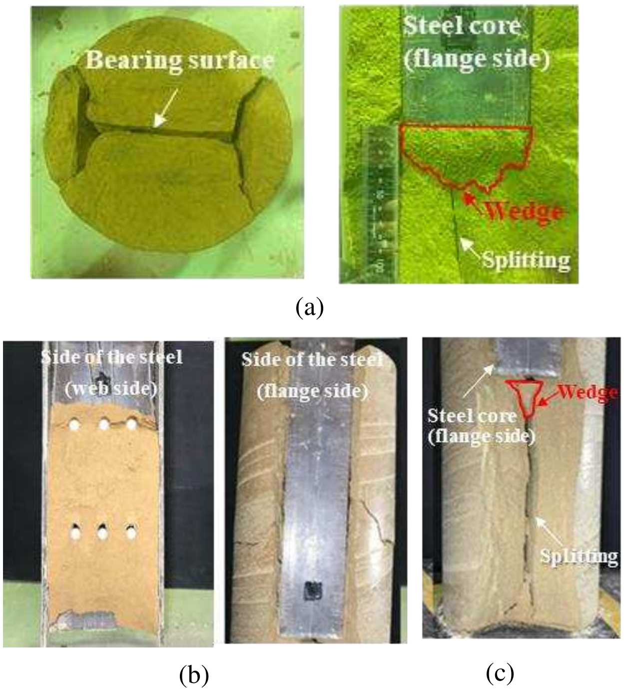

Figure 11. Failure behaviour of the model piles under unconfined conditions. (a) Wedge beneath the steel core tip (U_10C0, non-studded pile), (b) Above the steel core tip (U_10C3, studded pile), (c) Wedge beneath the steel tip (U_10C3, studded pile).

developed beneath the web. Conversely, for studded piles, the soil–cement could be manually disassembled, and no stud deformation was detected (Figure 13(b)). Below the core steel tip, splitting cracks occurred beneath the web, and wedge formation was not clear (Figure 13(c)).

3.3 Effect of Ground Confinement

To evaluate the effect of ground confinement on P_P and P_R, normalised pile head loads $\overline{P_P}$ and $\overline{P_R}$ were defined to account for the strength variability of soil–cement, using Equations (1) and (2) based on the ratio of the unconfined compressive strength q_u to the target strength q_{u0}.

$$\overline{P_P} = P_P \cdot \frac{q_u}{q_{u0}} \quad (1)$$

$$\overline{P_R} = P_R \cdot \frac{q_u}{q_{u0}} \quad (2)$$

Figure 14 shows the relationships between $\overline{P_P}$, $\overline{P_R}$, and the overburden pressure p_0. For $\overline{P_P}$, the influence of overburden pressure was minor for non-studded piles. In contrast, for studded piles, TL_10C3 exhibited approximately 1.1 times higher values and TM_10C3 about 1.3 times higher values compared with U_10C3.

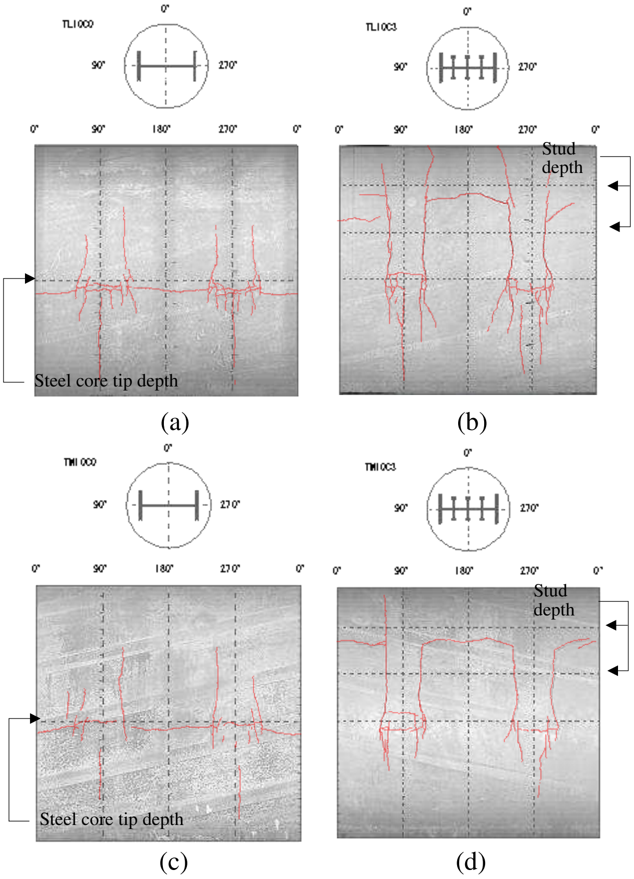

Figure 12. Crack sketches of model piles under confined conditions. (a) Non-studded pile (TL_10C0, p_0=50kPa), (b) Studded pile (TL_10C3, p_0=50kPa), (c) Non-studded pile (TM_10C0, p_0=100kPa), (d) Studded pile (TM_10C3, p_0=100kPa)

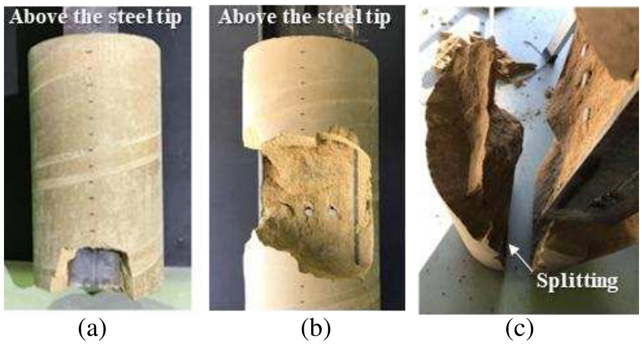

Figure 13. Failure behaviour of the model piles under confined conditions (p_0=100kPa).(a) Above the steel core tip (TM_10C0, non-studded pile), (b) Above the steel core tip (TM_10C3, studded pile), (c) Splitting failure (TM_10C3, studded pile).

$\overline{P_R}$ exhibited a more pronounced dependence on overburden pressure than $\overline{P_P}$. For non-studded piles, TL_10C0 and TM_10C0 showed approximately 5.4 and 7.8 times higher $\overline{P_R}$ than U_10C0, respectively.

For studded piles, TL_10C3 and TM_10C3 exhibited about 9.1 and 11.5 times higher values than U_10C3.

When the maximum values were compared, the influence of overburden pressure on non-studded piles remained minor. However, for studded piles, TL_10C3 and TM_10C3 exhibited approximately 1.3 and 1.6 times higher values respectively, than U_10C3, confirming that the confining effect becomes more significant with the installation of studs.

The results showed that ground confinement had a limited effect on non-studded piles but enhanced peak and significantly residual capacities of studded piles. This difference is attributed to changes in failure mode and load transfer mechanism induced by stud installation.

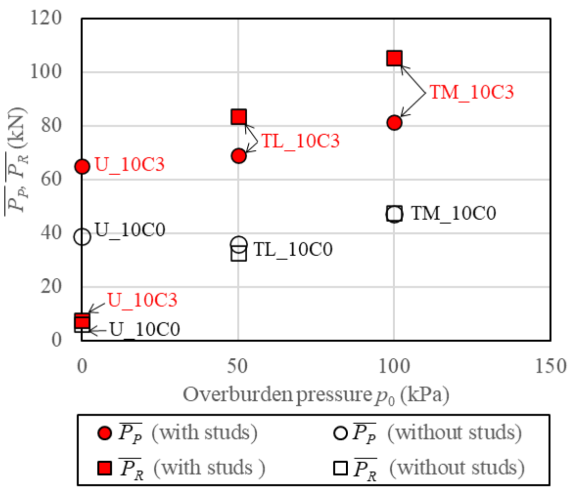

Figure 14. Relationship between $\overline{P_P}$, $\overline{P_R}$ and overburden pressure p_0.

4 CONCLUSIONS

Vertical loading tests on soil–cement H-shaped steel piles using a pressurised soil chamber were conducted to investigate the effects of headed stud installation and ground confinement on the vertical bearing capacity. The main findings are summarised as follows:

1. The resistance provided by headed studs was progressively mobilised with increasing displacement, resulting in an increase in pile head load up to a displacement of 10% of the pile diameter under confined conditions.
2. The installation of headed studs altered the failure mode of the soil–cement from bond-dominated failure to combined bond-shear failure, thereby improving the mechanical integrity between the steel core and the surrounding soil–cement.
3. Ground confinement significantly enhanced the vertical bearing capacity, and this enhancement became more pronounced when headed studs were installed, due to differences in failure mode and load transfer mechanism.

Future studies will focus on quantifying the confining effects on individual resistance component—namely, bond resistance and shear resistance along the steel core shaft, the tip bearing resistance and the stud resistance—in order to establish a rational method for evaluating the vertical bearing capacity of soil cement H-shaped steel piles.

It should be noted that the present study was conducted under pressurised soil chamber conditions with a uniform confining pressure. The tests were conducted on model piles focusing on the region near the tip of the steel core at a model scale of 1/2.5. In actual ground conditions, the confining pressure increases with depth, and full-scale structures may exhibit scale-dependent behaviour. Therefore, full-scale in-situ loading tests would be beneficial to confirm the applicability of the present findings to field conditions.

REFERENCES

Architectural Institute of Japan (2017). AIJ Recommendations for Design of Earth Retaining for Excavation, pp.130-133. (in Japanese)

Kiritani, R., Shimomura, S., Aoyama, A., and Nomura, Y. (2025). Study on the confinement effect of ground on the vertical bearing capacity of soil–cement retaining wall using model tests, *Journal of Structural and Construction Engineering, Architectural Institute of Japan*, Vol. 90, No. 829, pp.354-364. (in Japanese)

Mano, H. and Abe, K. (2018.). Bearing capacity of H-shaped steel in soil cement retaining wall (Part 2:Evaluation for stud resistance to soil cement), *The 53rd Japan National Conference on Geotechnical Engineering*, pp.1433-1434. (in Japanese)

Satake, K., Uchii, E., Otsuka, S., Fujiwara, T. and Takeuchi, Y. (2003). Development of a permanent soil cement mixing pile, Part 4 Transmission of load between soil cement & H-Steel, *Summaries of Technical Papers of Annual Meeting, Architectural Institute of Japan*, Structure-I, pp.677-678. (in Japanese)

Taya, Y. and Yamanaka, R. (2021). Evaluation for adhesion of H-section steel and stud resistance to soil-cement by trench cutting re-mixing deep wall method, *Summaries of Technical Papers of Annual Meeting, Architectural Institute of Japan*, Structure-I, pp.365-366. (in Japanese)

Watanabe, K., Wada, K., Yokoyama, T. and Hirata, M. (2021). Evaluation of bond performance on pile body of soil-cement mixing wall used as permanent pile, *Journal of Structural Engineering*, Vol.67B, pp.445-452. (in Japanese)